HEFAT2012
9th International Conference on Heat Transfer, Fluid Mechanics and Thermodynamics
16 – 18 July 2012
Malta

EXPERIMENTAL CHARACTERIZATION OF COMBUSTION IN RECIRCULATION ZONE OF DOUBLE-STAGE SWIRL CHAMBER

Tessele, S.G.[1]*, Almeida, D.S.[1], Barreta, L,G.[2], Sbampato, M.E.[2], Martins, C.A.[1], Lacava, P.T[1*]
*Author for correspondence
[1] Department of Aeronautical Engineering,
Aeronautical Institute of Tecnology, ITA,
São José dos Campos, Brazil
[2] Institute for Advanced Studies, IEAv.
São José dos Campos, Brazil
e-mail: placava@ita.br

ABSTRACT

The focus of the present work is a new Low-NO_x combustor configuration to especial application in gas turbine. The combustion happens in two phases; the first one with oxidant deficiency, or fuel rich combustion, and the second one is a fuel lean combustion. This combustion structure allows the conciliation of low NO_x emissions and partial oxidation combustion products, as carbon monoxide and unburned hydrocarbons. In the new concept proposed here, these unfavorable combustion conditions for NO_x formation are reached through the dynamic control of reactants mixing process into the chamber. However, the success of this strategy depends on the formation of a strong recirculation zone in the secondary chamber and quick-mixing between air, reminiscent fuel and combustion products. So that the present work shows experimental results about the structure of the recirculation zone using Particle Image Velocimetry (PIV) and the combustion dynamics using Planar Laser Inducing Fluorescence (PLIF). Both techniques were applied in the secondary zone of combustion. The conclusion based on the results presented in this paper can be summarized according to the increase of the recirculation zone intensity: 1. the volume occupied by recirculation zone is greater, the transition to reverse flow is more abrupt and the magnitude of the reverse velocity is higher; 2. intensify the vortices formation; 3. the combustion reactions take place in the central region of recirculation zone.

INTRODUCTION

As result of the rapid increase of the air traffic and the large use of gas turbines to produce electric power, the reduction of pollutants has become the main objective in the design of gas turbine engines. To reduce CO_2, one of the most important causes of the greenhouse effect, the tendency of the advance combustion chamber is to increase not only the inlet pressure and temperature but also the efficiency of the engine and to reduce the fossil fuel consumption. For aircraft gas turbines this is the only way to reduce CO_2 emission. However, it increases the maximum temperature in the combustor and more NO_x is produced. In this way, some efforts have been made to develop technologies to control NO_x emissions for high performance gas turbines.

Lean premixed combustion, which has high reliability, minimal impact on turbine performance, and low emissions, is now an accepted technology for stationary gas turbine engines [1]. This allows the NO_x reduction by reducing the equivalence ratio in the combustion zone and consequently the reduction of flame temperature peak [2]. Unfortunately, however, lean premixed combustion systems are highly susceptible to dynamic instabilities, which lead to severe problems, such as a shortened lifetime of the overall system and an unstable operation with harmful emissions [3]. Moreover, another difficulty often encountered in practical combustion devices is the premature auto-ignition of fuel/air mixture before it reaches the main combustion zone [4].

Another technology to control NO_x formation in gas turbine combustors is the Rich-Quench-Lean combustion – RQL. The RQL combustor designs incorporate an axially-staged approach in which the air injection is staged axially along the axis of the combustor. Although fuel-bound nitrogen species are converted to NO_x very efficiently in an oxidizing environment [5], if the nitrogen-bearing fuel is injected into a fuel-rich environment, a significant portion of the fuel-bound nitrogen species will be converted to N_2, instead of NO_x. Once complete oxidation does not occur in the rich zone of a RQL combustor, additional oxidant is required to complete the combustion at an overall lean condition. The point at which this additional oxidant is injected is often called the quick-mix stage of an RQL combustor [6]. This mixing zone is critical for minimizing thermal, or Zeldovich, NO_x production; the air injected into the mixing zone should mix quickly and homogeneously and this is the main difficulty to design RQL combustors. In addition, in

the rich zone considerable quantity of soot is formed, increasing dramatically the heat transfer by radiation to the combustor wall. Then, some complex system of air film cooling should be present.

In fact, there are some improvements in LP and RQL original concepts to produce combustion devices with extremely low NO_x emissions. For example: Lean Pre-mixed Burner with Spatially Periodic Recirculation of Combustion Products [7], Double Swirler Lean Premixing Pre-vaporizing Burner [8], Rich-Burn, Quick-Mix, Lean-Burn Trapped Vortex Combustor [6], Rich-Catalytic Lean-Burn Combustion [9]. Combinations of combustion zones unfavorable for NO formation and favorable to conversion of fuel-bound nitrogen to N_2 are the most important way to control NO_x emissions by the modifications in the combustion process.

In particular, the present paper is concerned about the combustion dynamics in a two phases swirl combustor. This combustor configuration uses part of RQL and LP concepts to control NO_x emissions; however, without premixing in a preliminary duct as the LP combustors and without staged air addition as the RQL combustors. The combustion zones unfavorable to NO formation are established by the flow dynamic of the reactants and the burned gases into the chamber. Basically the combustor has two stages or two combustion chambers. In the first one, the total air flow emerges in a cylindrical chamber through a swirler; consequently, an intense circular flow with high tangential velocity takes place around the primary chamber wall. The fuel is injected in the primary chamber center line, and a yellow sooting flame is observed in the region of interaction between the fuel jet and the air circular flow. The air flow absorbs the intense heat transferred by radiation from the sooting flame and acts as a natural film cooling. In the transition region for the first to the second chamber, there is an abrupt increase of the combustor diameter and part of the air from the first chamber reverts to the chamber center line, creating an intense recirculation zone, which is responsible for the quick-mix between the air, reminiscent fuel and combustion products. It is clear that the success to control NO_x emissions depends on the main controlling parameters of the flow dynamic into the combustor, which are: the intensity of the air tangential velocity in the first stage, the Reynolds number of fuel jet injection, the ratio length/diameter of the first stage and the global equivalence ratio.

The success of this strategy depends on the formation of a strong recirculation zone in the secondary chamber and quick-mixing between air, reminiscent fuel and combustion products. So that the present work shows experimental results about the structure of the recirculation zone using Particle Image Velocimetry (PIV) and the combustion dynamics using Planar Laser Inducing Fluorescence (PLIF). Both techniques were applied in the secondary zone of combustion.

EXPERIMENTAL SETUP

The experiments were performed in an atmospheric pressure laboratorial scale combustor, made in stainless steel and without refrigeration. As commented before, the air flow acts like a film cooling and the refrigeration is not necessary. The original combustor has a primary chamber diameter (D) of 10 cm and the length (L) may be 10, 20 or 30 cm (L/D ratio = 1, 2 or 3), for the secondary chamber the length and the diameter are 50 and 40 cm, respectively. The air, which comes from the air blowers, is conducted axially to the swirler positioned at the primary chamber entry. The swirler diameter is the same of the primary chamber; it has eight blades and the angle with the axial direction may be set from 0° to 80°. The Figure 1 shows a schematic diagram of the experimental setup.

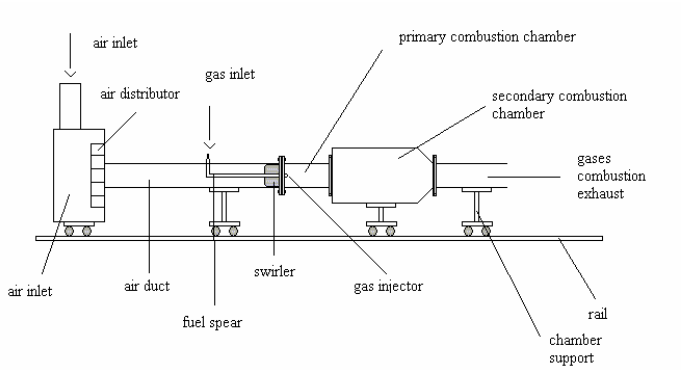

Figure 1 Schematic diagram of the experimental setup

The mass flow rate of the natural gas was kept constant at 1 g/s for all experiments, and maximum air mass flow rate was 100 g/s. Both mass flow rates were measured by calibrated orifice plate systems and the maximum error is 3% of the measure. The fuel was injected through the nozzle positioned in the center line of the primary chamber. Three different nozzle diameters may be used, 2.35, 3.20 and 7.8 mm, to provide the fuel jet Reynolds numbers of 50,000, 40,000 and 15,000, respectively.

The parameters that may be changed during the experiments were: L/D ratio for the primary chamber, fuel jet Reynolds number (Re), swirler blades angle (α) and the global equivalence ratio (ϕ). As commented before, two different regions of combustion are observed into the combustor. Into the primary chamber, a cylindrical sooting flame is observed and after a quick transition, an intense blue flame is present in the secondary chamber. To illustrate it, Figure 2 shows a photo where the stainless steel primary chamber is substituted by a cylindrical glass chamber and the secondary chamber is not present. The operation conditions for the photo presented in Fig. 2 are: natural gas mass flow rate $\dot{m}_F$ = 1.0 g/s, air mass flow rate $\dot{m}_{air}$ = 50 g/s, swirler blades angle $\alpha = 80^o$ and L/D = 1. Table 1 summarizes the experimental conditions.

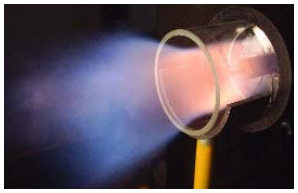

Figure 2 Two-stage experimental swirl flame

Table 2 Summary of experimental conditions

Primary chamber length	10 cm
Primary length/diameter ratio (L/D)	1, 2 and 3
Secondary chamber diameter	40 cm
Fuel mass flow rate	1 g/s
Global equivalence ratio	0,15 – 0,45
Swirler angle (α)	40^o – 80^o
Fuel jet Reynolds number (Re_p)	15,000, 40,000 and 50,000
Condition of intake air	25^oC and 1 bar

The success of this strategy depends on the formation of a strong recirculation zone in the secondary chamber and quick-mix between air, reminiscent fuel and combustion products. Thus, two laser techniques for diagnostic were used, Particle Image Velocimetry – PIV and Planar Laser Inducing Fluorescence – PLIF, to better understand the combustion dynamics, especially close to recirculation zone. Both techniques were applied to visualization just the recirculation zone, which is the focus o present paper. The secondary chamber was removed and the experiments were conducted in a non-confined secondary zone of combustion for a better optical assessment. However, the results are consistent with the confinement situation, at least qualitatively.

The presence of the secondary chamber wall evidently has some influence on the flow dynamic; but in practical combustor of gas turbine the liner diameter has at least three times the swirler diameter to reduce the wall interference in the recirculation zone. So that, as mentioned before, at least qualitatively the present results are consistent with confined situation, because secondary chamber diameter is four times the swirler diameter.

PIV is a quantitative technique for measuring the instantaneous velocity field of fluid mechanic experiments. This technique consists on adding tracer particles to the flow; then the particles will follow the flow during its trajectory. The particles are illuminated by two laser pulses during an established time interval; then, a pair of images is obtained and is stored by a high-resolution CCD camera (*Charge Coupled Device*). After the images post-processing, the velocity field is obtained. The setup used here for PIV measurements was: a Laskin *nozzle* oil droplet generator with output pressure of 1.5 bar and droplets diameter in the range of 1-2μm, a twin ultra double cavity Nd:YAG laser system comprised by two laser heads with beam combining optics, a cylindrical lent to create the laser shit and a high performance digital 12bit CCD camera system. It was also used a synchronism laser software, it controls the laser parameters and synchronizes the trigger signals with the activation of the CCD camera. Basically, the digital PIV recording is divided into small sub-areas called "interrogation areas", where it is obtained the local displacement vector of the tracer particles for the images of the first and second illumination. It is determined by means of statistic methods (cross-correlation). Some filters were used to improve the quality of results, which means to identify and to remove spurious vector in relation to neighboring vectors. The filters used are based on the suggestion of Keane and Adrian [10] and Westerweel e Gharib [11] of The frequency of PIV measurements were 9 Hz. Figure 3 shows the experimental setup for PIV measurements. The tests were realized for non-reactive flow and fuel was simulated using compressed air.

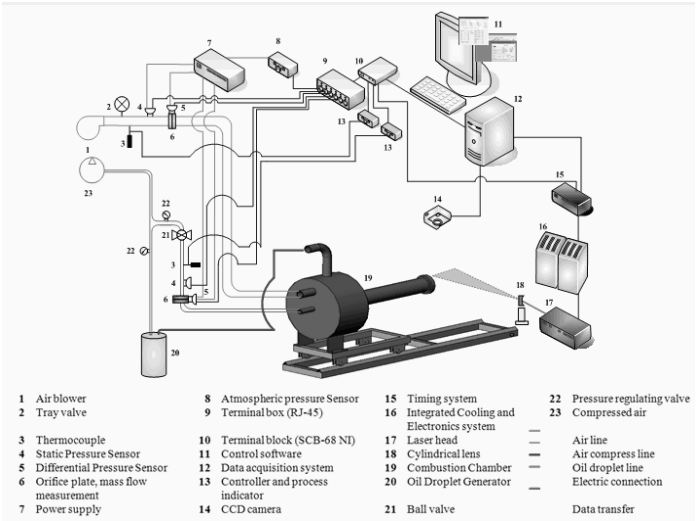

Figure 3 Experimental setup for PIV measurements.

The PLIF technique was used in the present work to detect the presence of OH radical, soot presence and fuel presence in the combustion recirculation zone. This technique uses one or more lasers to excite a determined state of a molecule or radical and to produce selectively an excited stated of the species desired to be monitored. If the life time of the species excited state is short compared to the collisional deactivation processes, the excited state will decay to a more stable state by fluorescence. This usually occurs at the fluorescence wavelength of the UV-visible and can be detected using photomultiplier tubes or ICCD camera. The intensity of fluorescence emitted is, in general, proportionally to the concentration of this species. Such systems are composed of three basic components:

1 - A dye laser (pumped excimer laser or Nd-Yag laser with frequency-doubled or tripled) or, in specific applications, a Nd-Yag laser with quadrupled frequency.

2 – A conditioner laser beam that transforms the cylindrical beam on a beam plan with reduced thickness. This is achieved through an appropriate system of cylindrical and spherical lenses.

3 – An ICCD camera for fluorescence detection and capture of images formed by the interaction of the laser beam with the system under study

For the present study, it was used a dye laser of Sirah, pumped by a Nd: YAG laser Quanta Ray INDI 10 Hz, with a double and triple of frequency, and a grid of 2400 lines. The energy emission was 460 mJ at 1054 nm, 240 mJ at 532 nm (crystal doubler) and 140 mJ at 326 nm (crystal tripler), suitable for working with flames. For the case of OH radical analyses, the laser pumping at 532 nm radiating Rhodamine 6G dye was used. Again, the experiments of OH-PLIF were conducted in non-confined combustion, i.e., without a secondary combustion chamber.

FORMATION OF RECIRCULATION ZONE

First of all, it is important to define the swirl number, which is the non-dimensional relation that can be use to quantify the swirl effect imparted by the swirler blades. It represents ratio between the flux of angular momentum (G_ϕ) and the flux of linear momentum (G_x). According to Lawn [12], both fluxes of momentum are conserved.

$$G_\phi = \int_{R_1}^{R_2} 2.\pi.\rho.u.w.r^2 dr = const. \quad (1)$$

$$G_x = \int_{R_1}^{R_2} 2.\pi.r.(p + \rho.u^2).dr = const. \quad (2)$$

where u and w are the axial and tangential components of velocity, respectively, in a transversal section limited by the radius R_1 and R_2, ρ is the density and p is the static pressure. Thus, the swirl number is calculated as:

$$S = \frac{G_\phi}{R.G_x}, \quad (3)$$

in general, R is $R_2 - R_1$. Using this model and right values for flows conditions and for swirler geometry, its possible classifies how each parameter influences the recirculation zone. For values higher than one, the recirculation zone is considered strong.

Swirler angle: basically increasing the swirler angle (α) the tangential momentum imparted by the swirler blades to the air flow also increase, which means that the recirculation zone will be stronger in the secondary zone. By proceeding calculations using the swirl number model presented before, it is possible to notice that the swirl number increases exponentially with the swirler angle.

Fuel jet Reynolds number: as mentioned before, this parameter is calculated based on the fuel nozzle diameter. In spite of increasing turbulence, the major effect, when fuel mass flow rate is kept constant and the fuel nozzle diameter is modified, is the axial momentum in the transition region between primary and secondary chambers. Just to have an idea, for the Reynolds numbers 15,000, 40,000 and 50,000, the fuel jet axial momentum flux in the fuel nozzle exit are 45, 259 and 497 $g.m.s^{-2}$. It is evident that the flow velocity through the primary chamber is reduced and the axial momentum at the chambers transition region is quite lower when compared with values in the fuel nozzle; however, any increase of the axial momentum in the transition region makes a weaker recirculation zone in the secondary chamber.

Combustor length/diameter in the primary chamber: in this case, when the length of primary chamber increases, the axial momentum in the transition region decreases, as consequence of the continuous reduction of fuel jet velocity in the primary chamber. So that, the "destruction" effect of the recirculation zone imparted by the central jet is minimized and the structure of recirculation zone stronger.

Global equivalence ratio: the reduction of the global equivalence ratio, which means for the present study increasing the air mass flow rate through the swirler blades, also intensifies the structure of recirculation zone. In the swirl number model presented, this parameter has a linear behavior with air mass flow rate.

RESULTS

It is important to inform that the comments made in the previous sections agree with the results from PIV studies in the recirculation zone without combustion. There is a collection of results and it does not make sense to present all data here due to the qualitative behavior when each parameter changes to make the recirculation zone stronger. So that, just one representative example is given, in this case all parameters were maintained constant and the two swirler blade angles were investigated, 60 and 80°, as presented in Figure 4.

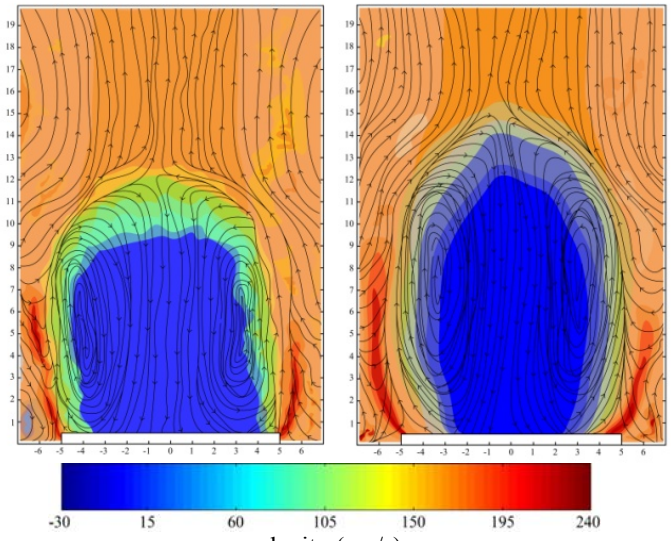

(a) Results for L/D = 1, α = 60°, Re_p= 40000 and air/fuel mass flow rate = 21.53.

(b) Results for L/D= 1, α = 80°, Re_p = 40000 and air/fuel mass flow rate = 21.01.

Figure 4 Recirculation zones PIV measurements. The scales in the axes correspond to the distances in cm.

The experiments were conducted under ambient average temperature of 28 ± 1°C, barometric pressure of 940 ± 1 mbar and relative humidity of 60 ± 1%. All acquisitions were made considering the actual velocity of the flow near the primary chamber, spatial resolution of 157.4 μm/pixel and mean velocity fields obtained from 50 pairs of images. The criterion to determine the number of pair of images was the rms value of the velocity; after approximately 40 pair of images the rms values stabilizes, then 50 pairs were considerate sufficiently good.

Analyzing the images of Figure 4, it is possible to note, for both cases α = 60 and 80°, the behavior of the flow is almost symmetrical to the longitudinal axis of the camera. The mean velocity fields indicate that part of the flow at the exit of the primary chamber experiments reverses velocities, when compared with other studied regions. This indicates the presence of a significant recirculation zone produced by the adverse gradient pressure in the axial direction [13,14]. According to Huang and Yang [15], the recirculation zone plays an important role for flame stabilization, due to the intensification of the mixing process as a consequence of the strongest recirculation zone.

Additionally, it is possible observe the circular and concentric stagnation region regarding the longitudinal axis of the combustion chamber and around this region there are lines featuring a circular pattern, characterizing a vortical structure. Also note that the flow direction is from inside the central zone and movement to its borders. This vortical structure emerges from the interaction between the recirculation zone and the flow that develops inside of it.

Qualitatively, the mean velocity fields presented in Figure 4 have the same structure; however, some important differences may be noted when the swirler angle increases and the recirculation zone becomes stronger. The swirl number for α = 60° e 80° for the PIV tests showed in Figure 4 were 3.19 and 29.27, respectively, calculated using the model presented before. Both conditions have a well-defined circulation zone, but for the smaller swirl number the velocity magnitude transition between the region inside and outside of recirculation zone was more gradual than the highest swirl number. This transition may be best viewed through the succession of colors representing the velocity ranges; for example, for 60° in Figure 4, when the flow reverts, it is possible to observe a smooth velocity change by the gradual color change from orange to dark blue. However, for 80°, the change is not gradual; rapidly the flow reverts to low or negatives values of velocity. Also, the increase of swirl number produces a more uniform boundary between flows (reduction wave at the border) and a larger structure of recirculation with magnitudes of a more intense reverse flow (about -20cm/s) compared with those recorded for α = 60° (about - 5cm /s).

It is important to keep in mind that the results of Figure 4 are the mean behavior of instantaneous images, and the mean recirculation zone is the mean behavior of a temporal sequence of formation, propagation and destruction of vortices. Figure 5 shows two representative instantaneous velocity fields for both conditions presented in Figure 4. It is clear that production of vortices and their propagation are more intense for higher swirl number. Furthermore, the literature reports this formations of vortices as a Kelvin-Helmholtz instability in the shear layer and are thus a product of the mean flow field.

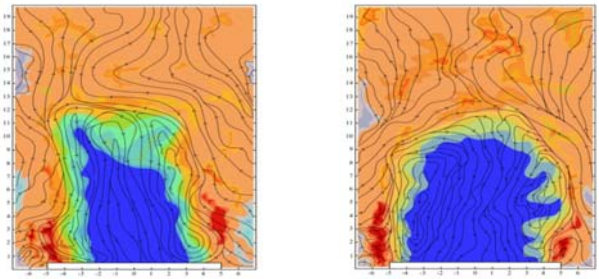

(a) Results for L/D = 1, α = 60°, Re_p= 40000 and air/fuel mass flow rate = 21.53

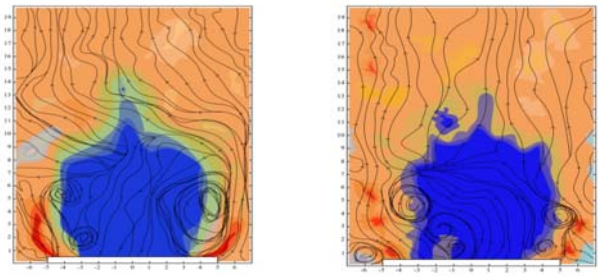

(b) Results for L/D= 1, α = 80°, Re_p= 40000 and air/fuel mass flow rate = 21.01.

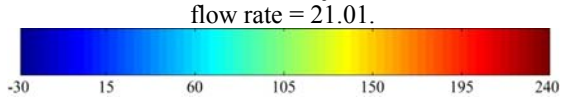

velocity (cm/s)

Figure 5 Instantaneous velocity fields. The scales in the axes correspond to the distances in cm.

For PLIF investigations 54 different flames conditions were studied changing the swirler angle, the fuel jet Reynolds number and the combustion air mass flow rate. Just to exemplify the flame confinement into the recirculation zone, results are presented in Figure 6 for the case: swirler angle 60°, first stage combustor length 0.2 m, fuel mass flow rate 1.0 g/s, combustion air mass flow rate 50 g/s and fuel jet Reynolds number 40,000. Figure 6 shows the results for the flame stabilized close to the recirculation zone: (a) flame picture, (b) OH-PLIF, (c) PIV result for non-reactive flow, (d) acetone-PLIF for non-reactive flow and simulating the fuel distribution into recirculation zone, (e) soot presence-PLIF and (f) soot presence-PLIF normalized.

The Figure 6 (a) presents a flame picture just after primary duct and mainly confined close to the recirculation zone. The image (b) represents the results of PLIF technique for the radical OH. This radical is important intermediary specie during the hydrocarbon combustion and in general indicates the region of more intense concentration of combustion reactions. To obtain the OH image, the laser was adjusted to the wave length of 282 nm and to better visualize the radical presence the image (b) is a sum of 200 images taken by ICCD camera.

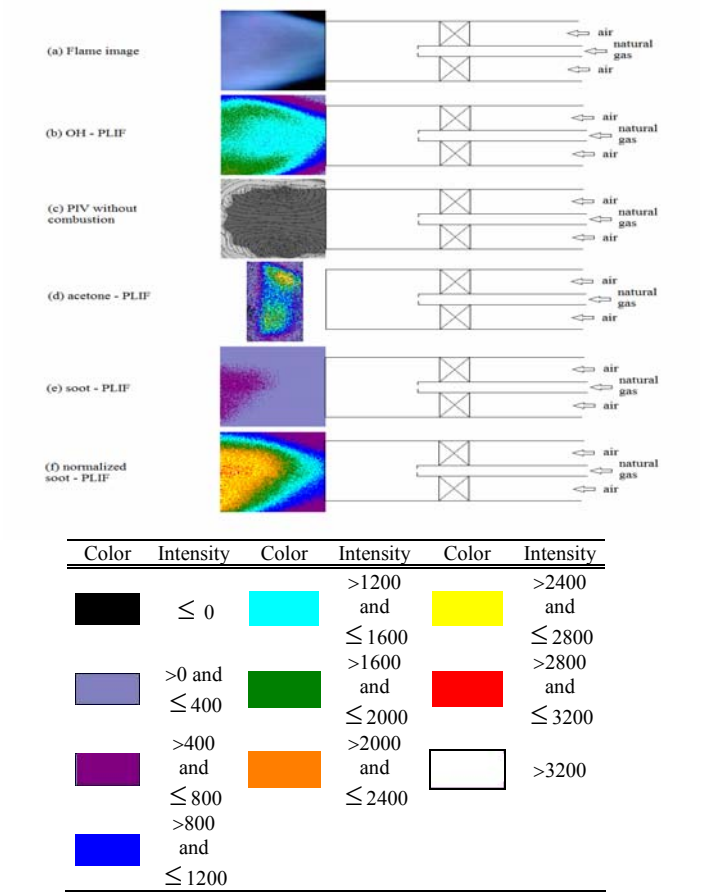

Color	Intensity	Color	Intensity	Color	Intensity
	≤ 0		>1200 and $\leq$1600		>2400 and $\leq$2800
	>0 and $\leq$400		>1600 and $\leq$2000		>2800 and $\leq$3200
	>400 and $\leq$800		>2000 and $\leq$2400		>3200
	>800 and $\leq$1200				

Figure 6 Recirculation zone observation for different techniques (arbitrary intensities).

Comparing the OH image with the result for average velocity field (image c), it is observed that the most of reactions are confined in the recirculation zone; however, they are not exactly in the central region, but preferably concentrated between the stagnation zone and the external undisturbed flow, which is the shear layer between the reversed flow and undisturbed flow. It makes sense if compared with the image (d) for non-reactive flow PLIF of acetone. In this case a jet of compressed air with acetone simulates the fuel flow. The objective of acetone PLIF is to understand the dynamic of fuel flow in the recirculation zone. The image (d) corresponds to a sum o 40 images taken by ICCD camera. Note that there is a high concentration of fuel confined in the central region of recirculation zone. It helps to explain the most of combustion reaction in more external regions, as presented in OH-PLIF, where there is greater possibility of mixtures formation and continuous ignition. Additionally, the soot-PLIF images (Figures 6 (e) and 6 (d)) shows that most of soot presence happens in the internal part of the recirculation zone. The chemistry and physics of soot formation in flames are exceedingly complex, but they (chemistry and physics) can be summarized in four steeps: 1) formation of precursor species (polycyclic aromatic hydrocarbon – PAH); 2) particle inception; 3) surface growth and particle agglomeration; 4) soot oxidation. For more details of soot formation in combustion, Glassman [16] provides a general review. In spite of the complex mechanism of soot formation and oxidation, works as Santoro et al. [17] have shown that the soot formation in flames occurs in a very narrow region and confined to a restrict range of temperatures 1300 – 1600K, in the inner zone between the flame and center line, where the oxidant concentration is close to zero and exposed to the bath of species from pyrolizing fuel. At some instant, the soot particle can pass through an oxidizing region of the flame. Therefore, the total soot emission is the difference between the soot formed in the flame inner region and soot oxidized in the flame. The soot-PLIF images in Figures 6(e) and 6(f) make sense, because, as presented by acetone – PLIF, in the internal part of the recirculation zone there are large quantities of fuel and probably also combustion products, providing conditions of temperature for soot presence in this region.

Several experiments were conducted to observe the radical OH when the recirculation zone becomes stronger. Again, it does not make sense to present all results and just a representative example is observed here; in this case, all parameters were maintained constant and three swirler blades angles were investigated, 60, 70 and 80°. However, a qualitative behavior for flame stabilization is expected when one parameter is changed to make the recirculation zone stronger. Figure 7 presents the results for OH – PLIF for L/D= 1, α = 60, 70 and 80°, Re_p = 40,000 and air/fuel mass flow rate = 21.01. The laser wave length was adjusted to 282 nm, the images are the sum of 200 images obtained by a ICCD camera.

Back to the image presented in Figure 2, it is possible to note that the blue flame of the secondary phase of combustion is stabilized in the front of the primary chamber duct exit and involved by the recirculation zone. For $\alpha = 60^o$ in Figure 7, if compared with non-reactive results of PIV measurements in Figure 4, it is observed that most of reactions are confined close to the recirculation zone, but not exactly in the central region, where the reminiscent fuel is injected (it is confirmed by acetone – PLIF injected in the fuel flow, as commented before). When the swirler angle increases, there is a tendency of concentrating the reaction in front of the primary chamber exit, i.e., in the central region of recirculation zone, where, for lower swirl numbers, for example 3.19 for $\alpha = 60^0$ in Figure 6, just fuel and products were present. Thus, it possible to point out that the intensification of recirculation zone concentrated combustion reactions, increasing the rate of combustion in the secondary zone (energy released per unit of time and volume).

However, although the symmetrical toroidal recirculation zone presented in Figure 4, the distribution of combustion reactions is not symmetric in the recirculation zone (Figure 7). It happens because the flame is following the trend of the flow that emerges tangentially from the primary chamber at a specific point. So that the flame stabilization depends on: the intensity of the recirculation zone and the tangential momentum when the air flow emerges from the primary chamber. Additionally, it is clear that increasing drastically the intensity of recirculation, for example, for 80°, the magnitude order for swirl number is 30, whereas for 60° is 3, the flame

stabilization migrates to central zone of recirculation zone, not only in the shear layer as observed for 60°. Probably the stronger recirculation captures more oxygen and products to the central region, then providing conditions of flammability and for ignition. This final comment is just as speculation, because is not proved here.

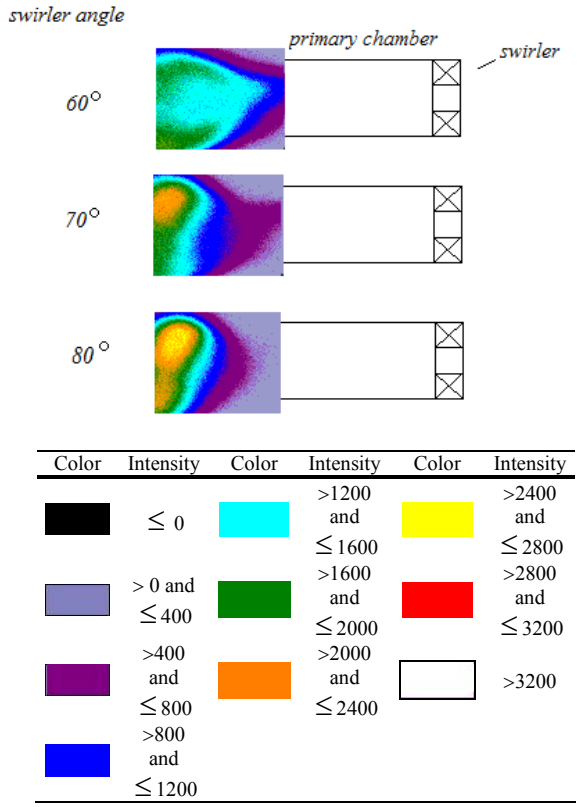

Figure 7 OH distribution using PLIF technique for different conditions of recirculation zone intensity (arbitrary intensities).

CONCLUSIONS

The present paper experimentally investigated the structure of recirculation zone using PIV and PLIF optical techniques. PIV was utilized to characterize the average velocity field in the recirculation zone and vortices formation and dissipation. Additionally, PLIF was utilized to observe the OH radical and the soot for combustion situations and to observe fuel dissipation flow into de recirculation zone, acetone-PLIF, for non-reactive flow.

The results presented in this paper can be summarized according to the increase of the recirculation zone intensity: 1. the volume occupied by recirculation zone is greater, the transition to reverse flow is more abrupt and the magnitude of the reverse velocity is higher; 2. Intensify the vortices formation; 3. the combustion reactions take place in the central region of recirculation zone. These observations are important to be associated with others studies about pollutant emissions in this configuration of combustor.

Based on the results, the practical conclusion for design recommendations is to adjust the parameters that control the recirculation structure, for example, swirler angle, fuel jet Reynolds number, length of primary chamber, etc., to provide an intense recirculation region in the secondary chamber. The effect of each parameter is cited in section "Formation of Recirculation Zone".

REFERENCES

[1] Cho, E. S. and Chung, S.H., 2009, "Improvement of Flame Stability and NO_x Reduction in Hydrogen-Added Ultra Lean Premixed Combustion", Journal of Mechanical Science and Technology, Vol. 23, pp. 650-658.

[2] Kang, D.M., Culick, F.E.C. and Ratner, A., 2007, "Combustion Dynamics of a Low-Swirl Combustor", Combustor and Flame, Vol.151, pp. 412-425.

[3] Hong, J.G., Oh, K. C., Lee, U.D. and Shin, H.D., 2008, "Generation of Low-Frequency Alternative Flame Behaviors in a Lean Premixed Combustor", Energy and Fuels, Vol. 22, pp. 3016-3021.

[4] Gokulakrishnan, P., Gaines, G., Currano, J., Klassen, M.S. and Roby, R.J., 2007, "Experimental and Kinetic Modeling of Kerosene-Type Fuels at Gas Turbine Operating Conditions", Journal of Engineering for Gas Turbine and Power, Vol. 129, pp. 655-663.

[5] Sarv, H., and Cernansky, N. P., 1989, ''NO_x Formation From the Combustion of Monodisperse n-Heptane Sprays Doped With Fuel-Nitrogen Additives", Combustion and Flame, 76, pp. 265–275.

[6] Straub, D.L., Castelon, K.H., Lewis, R.E., Sidwell, T. G., Maloney, D.J., and Richards, G.A., 2005, "Assessment of Rich-Burn, Quick-Mix, Lean Burner Trapped Vortex Combustor for Stationary Gas Turbines", Journal of Engineering for Gas Turbine and Power, 127, pp. 36-41.

[7] Kalb, J.R., and Sattelmayer, T., 2006, "Lean Blowout Limit and NO_x Production of a Premixed Subppm NO_x Burner with Periodic Recirculation of Combustion Products", Journal of Engineering for Gas Turbine and Power, 128, pp. 247-254.

[8] Canepa, E., Di Martino, P., Formosa, P., Ubaldi, M., and Zunino, P., 2006, "Unsteady Aerodynamics of an Aeroengine Double Swirler Leas Premixing Prevaporizing Burner", Journal of Engineering for Gas Turbine and Power, 128, pp. 29-39.

[9] Smith, L.L., Karim, H., Castaldi, M.J., Etemad S., Pfefferle, W.C., Khanna, V., and Smith K.O., 2005, " Rich-Catalytic Lean-Burn Combustion for Low-Single- Digit NO_x Gas Turbines", Journal of Engineering for Gas Turbine and Power, 127, pp. 27-35

[10] Keane, R. D., Adrian, R. J., 1992, "Theory of cross-correlation analysis of PIV images" Applied Scientific Research, v. 49, n.3, pp.191-215.

[11] Westerweel, D.D.J., Gharib, M., 1997, "The effect of a discrete window offset on the accuracy of cross-correlation analysis of digital PIV recording". Experiments in Fluids, v.23, n. 1, pp. 20- 28.

[12] Lawn, C.J., 1987, "Principles of Combustion Engineering for Boilers", New York, Academic, 628p.

[13] Coche, A., Solero, G. Scribano, G., 2004, "Recirculation Phenomena in a Natural Gas Swirl Combustor", Experimental Thermal and Fluid Science, v.1, n. 28, p. 706-714.

[14] Huang, Y., Yang, V., 2004, “Bifurcation of Flame Structure in a Lean-Premixed Swirl-Stabilized Combustor: Transition from stable to unstable flame”, Combustion and Flame, v.1, n. 136, p.383-389.

[15] Huang, Y., Yang, V., 2005, “Effect of Swirl on Combustion Dynamics in a Lean-Premixed Swirl-Stabilized Combustor”, Proceedings of Combustion Institute, pp. 1775-1782.

[16] Glassman, I., 1998, “Soot Formation in Combustion Process”, In Proceedings of Twenty-Secondy Symposium (International) on Combustion , Pittsburgh, p. 295.

[17] Santoro, R.J., Yeh T.T., Horvath, Semerjian H.G., 1987, “The Transport and Growth of Soot Particles in Laminar Diffusion Flames”, Combustion Sciense and Thecnology, n 53, pp. 89-115.